Overcome the challenge for intratumoral injection of STING agonist for pancreatic cancer by systemic administration Authors

Keyu Li, Junke Wang, Birginia Espinoza, Yirui Xiong, Nan Niu, Jianxin Wang, Noelle Jurcak, Noah Rozich, Arsen Osipov, Mackenzie Henderson, et al.

Title: Overcome the challenge for intratumoral injection of STING agonist for pancreatic cancer by systemic administration

Authors

Keyu Li[1,2,3,4#], Junke Wang[1,2,3,4#], Birginia Espinoza[1,2,3], Yirui Xiong[5], Nan Niu[1,2,3,6], Jianxin Wang[1,2,3,7], Noelle Jurcak[1,2,3,8], Noah Rozich[1,2,3,9], Arsen Osipov[1,2,3,10,11], MacKenzie Henderson[1,2,3], Vanessa Funes[1,2,3], Melissa Lyman[1,2,3], Alex B. Blair[1,2,3,9], Brian Herbst[1,2,3], Mengni He[1,2,3], Jialong Yuan[1,2,3], Diego Trafton[1,2,3], Chunhui Yuan[1,2,3,9,12], Michael Wichroski[13], Xubao Liu[4], Yuquan Wei[5], Lei Zheng[1,2,3,9,10*]

Affiliations

[1]Department of Oncology and the Sidney Kimmel Comprehensive Cancer Center, Johns Hopkins University School of Medicine, Baltimore, MD 21287; USA.

[2]The Pancreatic Cancer Precision Medicine Center of Excellence Program; Johns Hopkins University School of Medicine; Baltimore, MD 21287; USA.

[3]The Bloomberg Kimmel Institute for Cancer Immunotherapy; Johns Hopkins University School of Medicine; Baltimore, MD 21287; USA.

[4]Current affiliation: Department of General Surgery; West China Hospital; Sichuan University; Chengdu, Sichuan 610041; China.

[5]Current affiliation: State Key Laboratory of Biotherapy, West China Hospital, Sichuan University; Chengdu, Sichuan 610041; China.

[6]Current affiliation: Zhejiang Provisional People's Hospital, Hangzhou, Zhejiang; China.

[7]Current affiliation: The First-affiliated Hospital of Zhejiang University, Hangzhou, Zhejiang; China.

[8]Current affiliation: Lake Erie College of Osteopathic Medicine; Erie, PA 16509; USA.

[9]Department of Surgery; Johns Hopkins University School of Medicine; Baltimore, MD 21287; USA.

[10]The Multidisciplinary Gastrointestinal Cancer Laboratories Program, the Sidney Kimmel Comprehensive Cancer Center, Johns Hopkins University School of Medicine, Baltimore, MD 21287; USA.

[11]Current affiliation: Cedars-Sinai Medical Center, Los Angeles, CA 90048; USA.

[12]Current affiliation: Department of General Surgery, Peking University Third Hospital, Beijing 100191, China.

[13]Bristol Myers Squibb Co, Princeton, NJ 08648; USA.

[#] Keyu Li and Junke Wang contributed equally to this work and are co–first authors.

***Corresponding author:** Lei Zheng, The Johns Hopkins Kimmel Cancer Center, 1650 Orleans Street, CRB1 Room 351, Baltimore, Maryland 21231. e-mail: lzheng6@jhmi.edu.

Abstract

Objective: Due to the challenge for intratumoral administration, innate agonists have not made it beyond preclinical studies for efficacy testing in most of tumor types. Pancreatic ductal adenocarcinoma (PDAC) has a T-cell excluded or deserted tumor microenvironment. Innate agonist treatments may serve as a T cell priming mechanism to sensitize PDACs to anti-PD-1 antibody (a-PD-1) treatment.

Design: Using a transplant murine model with spontaneously formed liver metastasis and also the genetically engineered KPC mouse model that spontaneously develops PDAC, we compared the antitumor efficacy between intrahepatic/intratumoral and intramuscular systemic administration of BMS-986301, a next-generation STING agonist. Flow cytometry, Nanostring, and cytokine assays were used to evaluate local and systemic immune responses.

Results: The study demonstrated that administration of STING agonist systemically via intramuscular injection is equivalent or potentially superior to its intratumoral injection in inducing both effector T cell response and antitumor efficacy. Compared to intratumoral administration, T cell exhaustion and immunosuppressive signals induced by systemic administration were attenuated. Nonetheless, either local or systemic treatment of STING agonist was associated with increased expression of CTLA-4 in the tumors. However, the combination of a-PD-1 and anti-CTLA-4 antibody with systemic STING agonist demonstrated the antitumor efficacy in the KPC mouse spontaneous PDAC model. Our study also demonstrated the feasibility and antitumor efficacy of systemic administration of BMS-986299, a new NLRP3 agonist.

Conclusion: For the first time, our study supports the clinical development of innate agonists

via systemic administration, instead of local administration, for treating PDAC.

Keywords: pancreatic ductal adenocarcinoma; stimulator of interferon genes; innate immune agonist; STING; NLRP3; tumor microenvironment; immune checkpoint inhibitor; immunotherapy; systemic administration; intratumoral injection.

What is already known on this topic – Despite promising preclinical studies, innate immune agonists including STING agonists and NLRP3 agonists have not been tested in most of tumor types due to the difficulties associated with their intratumoral delivery.

What this study adds – This study compared between intratumoral and systemic administration of BMS-986301, a next-generation STING agonist and BMS-986299, a new NLRP3 agonist in the preclinical models of pancreatic cancer. Notably, systemic administration of STING agonist showed comparable or potentially superior effector T cell response and antitumor efficacy compared to intratumoral administration, with attenuated T cell exhaustion and immunosuppressive signals.

How this study might affect research, practice or policy – For the first time, this study supports the clinical development of innate agonists via systemic administration for treating pancreatic cancer. Supported by the results in this study, a phase 1 trial evaluating BMS-986301 intratumoral or systemic intravenous injection as monotherapy or in combination with nivolumab (PD-1 blockade) and ipilimumab (CTLA-4 blockade) in patients with advanced solid cancers has been initiated (NCT03956680).

Introduction

Recent research has highlighted the crucial role of the innate immune system in tumor immunosurveillance and the stimulation of antitumor immune responses[1]. This has led to the development of several small-molecule innate agonists as potential immunotherapeutics or vaccine adjuvants for different types of cancer[2]. However, despite promising preclinical studies, these agents have not been tested in most of tumor types due to the difficulties associated with their intratumoral delivery[3]. Overcoming this challenge is critical for the clinical development of innate agonists. Nonetheless, the potential benefits of using innate agonists as T cell priming agents continue to provide an impetus for the exploration of novel strategies to overcome the challenge for their delivery.

Stimulator of interferon genes(STING) is a transmembrane protein that is expressed in various endothelial, epithelial and hematopoietic cells. Upon activation at the endoplasmic reticulum and subsequent translocation to the Golgi, STING recruits and activates TANK-binding kinase 1(TBK1), which in turn phosphorylates and activates interferon regulatory factor 3(IRF3) and NF-kB transcriptional programs, resulting in the expression and release of pro-inflammatory type I interferons(IFNs) and cytokines[4, 5, 6]. Accumulating evidence has suggested that STING also possesses cell-intrinsic tumor suppressive activity[7]. The mechanistic underpinnings of the cyclic GMP-AMP synthase-STING pathway make STING agonists(STING-A) a promising adjuvant to cancer vaccines[8]. Numerous natural or synthetic STING-A as monotherapy or in combined with other treatments have also been tested in both pre-clinical studies and clinical trials across many cancer types[9, 10].

Synthetic cyclic dinucleotides(CDNs) were the first generation of STING-A that entered the clinical trial phase of drug development due to their structural versatility and ability to bind all prevalent allelic variants of human STING.

Pancreatic ductal adenocarcinoma(PDAC) is one of the most lethal malignancies due to its resistance to conventional therapies. PDAC and other non-immunogenic “cold” tumors do not respond to immune checkpoint inhibitors(ICIs) as monotherapy largely due to the lack of tumor-infiltrating effector lymphocytes [11, 12]. Published studies have demonstrated that intratumorally injected STING-A inflamed the tumor microenvironment(TME) of PDAC with an effector T cell infiltration and reduced tumor burden in the mouse model of PDAC[13]. However, despite these promising results at the preclinical phase, anti-tumor efficacies of STING-A have not been substantiated, largely due to the challenge of intratumoral delivery of such agents, which may have never reached therapeutic dose levels or never been tested in the appropriate disease indications.

BMS-986301 is a novel CDN-based, next-generation STING-A and has demonstrated a promising antitumor activity in the CT26 and MC38 subcutaneous tumor murine models, resulting in more than 90% of tumor regression compared to only 13% with the first-generation STING-A, ADU-S100. Similar results were observed with a single intratumoral administration of BMS-986301 in combination with an anti-PD-1 agent [14]. However, these previous studies were limited by the subcutaneously implanted tumors, which do not resemble the TME of human PDAC[15]. Therefore, this present study aims to deliver this

next-generation CDN-based STING-A systemically and compare its anti-tumor efficacy and elicited immune response with the intratumoral injection of this agent in a liver metastasis model of PDAC.

Methods

Mouse experiments

The mouse study was conducted in accordance with the guidelines established by the Animal Care and Use Committee of Johns Hopkins University. Female C57Bl/6 mice aged 6 to 8 weeks were purchased from Jackson Laboratories and maintained under the Institutional Animal Care and Use Committee(IACUC) guidelines. Third-party management was responsible for maintaining the IACUC mouse protocol.

STING-A(BMS986301, BMS) was dissolved into DPBS(Life Technologies) vehicle and administered to tumor-bearing mice either by intratumoral or intramuscular injection once a week at a dose of 5mg/kg starting on day 14, for a total of three doses. a-PD-1(BMS936558, BMS) and an IgG control(ab18443, BMS) were administered intraperitoneally twice weekly starting on day 14, for a total of five doses, at a dose of 10mg/kg.

NanoString

After the mouse was euthanized and the tumor was harvested, the tumor tissues were submerged into RNA-later(Invitrogen) to preserve the RNA. The total RNA was extracted from the whole specimen using the AllPrep DNA/RNA/Protein Mini Kit(Qiagen) according

to the manufacturer's instructions. The RNA was then equalized for NanoString hybridization using the Formulatrix Tempest. The murine PanCancer Immune panel codeset XT_PGX_MmV1_CancerImm_CSO, Cat#115000142), which contains 750 target genes along with housekeeping and negative/positive control probes, was used for the NanoString hybridization. The data obtained was then analyzed using NanoString nSolver 3.0 and an internally developed NanoString Data Analyzer Rshiny app(BMS). The samples were run on the NanoString MAX system reader, and the data was analyzed using various CRAN and Bioconductor packages such as dplyr, tidyr, and reshape2 to clean, reformat and match the sample annotations to the normalized data exported from NanoString nSolverV.3.0.

Additional methods are provided in the Supplemental Materials.

Results

Develop a mouse model to resemble the intratumoral injection of STING-A in metastatic cancer patients

To examine whether systemic administration of STING-A is equivalent or superior to intratumoral(IT) injection, we established two mouse models to compare these two routes of innate agonist administration. We first developed a model to resemble the IT injection of STING-A in patients with metastatic diseases. This liver metastasis model was developed by implanting 7.5 x 10^5 tumor cells of the KPC tumor cell line, derived from the PDAC of the Kras/p53/pdx1-Cre(KPC) mouse model, through the hemisplenectomy procedure and splenic vessel injection to form liver metastases(Fig.S1A). The mice in this model would uniformly

die from liver metastases if not treated[17]. The changes in the sizes of the metastatic lesions in the liver can be monitored by small animal ultrasonography. Liver metastases have been identified as potential sites for the IT administration of the first-generation STING-A to treat patients with PDAC. In this study, the liver metastases serve as the clinically relevant target tumors for IT administration of STING-A(Fig.1A).

Mice were also inoculated subcutaneously with the KPC tumor cell line to form subcutaneous(SubQ) tumors, not for the IT injection of STING-A, but for the abscopal effect to be examined. As shown in Fig.1B, sixteen mice per group were treated by control vehicles(negative control, NC), a-PD-1, STING-A, and STING-A+a-PD-1(Combo). A total of five doses of a-PD-1 was administered twice a week by intraperitoneal injection(IP), while the STING-A was given for three weekly doses by IT injection to mimic local treatment or intramuscular(IM) injection to mimic systemic treatment. Mouse survival was followed; the target liver metastatic lesion was measured by ultrasound; and the subQ tumors was measured by calipers twice a week. We did not observe any obvious sign of toxicity including bleeding, infection, paralysis, and weight loss as a result of IT injection of STING-A. However, we noticed small areas of liver necrosis around the injection sites at the necropsy of two mice(Fig.S1B). It should be noted that only approximately 35% of mice in the hemisplenectomy model harbored a liver metastasis feasible for IT injection.

The results(Fig.1C) showed that the tumor growth inhibition(TGI) rate of the target liver metastasis lesion was significantly increased in the STING-A and a-PD-1 combination

treatment group(maximum TGI=88.68±98.42%, $p < 0.05$) and the STING-A group(maximum TGI=69.38±73.94%, $p < 0.05$) as compared to the negative vehicle group. To investigate whether the local intratumoral injection of STING-A could induce the abscopal effect, we implanted subcutaneous tumors on the bilateral flanks of the liver metastasis mice model to mimic distant metastases. The TGI rate of bilateral SubQ tumors was also significantly increased in the combo group(maximum TGI=66.38±86.00%, $p < 0.05$) as compared with negative control(Fig.1D). Interestingly, the TGI in the distant SubQ tumors is bigger than that of the locally targeted liver metastatic lesion, supporting an abscopal effect from the STING-A and a-PD-1 combo treatment. Moreover, we compared the survival of liver metastasis mice in the above treatment groups and found that the combo treatment significantly prolonged survival comparing to the control treatment and the STING-A treatment(Fig.1E). Nevertheless, the combo treatment prolonged survival modestly without a statistical significance comparing to the a-PD-1 treatment. It is possible that the local intratumoral injection of saline may have caused inflammatory response which resulted in a small effect on priming the tumor for the a-PD-1 treatment. Nevertheless, the combo treatment significantly prolonged survival comparing to the control treatment and the STING-A treatment(Fig.1E).

STING-A in combination with anti-PD-1 antibody enhances effector T cells infiltration and CD103$^+$dendritic cells in both target liver metastatic lesions and non-target metastatic lesions

To understand the mechanistic basis of the enhanced anti-tumor activity of STING-A in

combination with a-PD-1, we performed flow cytometry analysis of the tumor infiltrating leucocytes(TILs) derived from the targeted liver metastasis in the same PDAC mouse model. As described in the dosing schema in Fig.1B, mice received the a-PD-1 on days 14 and 17, and the STING-A on days 14. On day 21, the mice were sacrificed and the implanted SubQ tumors as well as livers were harvested. TILs from the targeted liver metastatic lesion and the whole liver tissue excluding the targeted lesion were compared. Note that the whole liver tissue harvested on day 21 was diffusely infiltrated by non-target metastatic lesions. The results showed that the STING-A+a-PD-1 combo therapy significantly increased the infiltration of the $CD8^+$ and $CD8^+PD\text{-}1^+$T cells, but not the $CD4^+$ and $CD4^+PD\text{-}1^+$T cells in the target lesion comparing to treatment controls(Fig.2A;Fig.S1C). Interestingly, a-PD-1, STING-A, or their combo all decreased the $MHCII^+CD11c^+$dendritic cells(DCs); however, comparing to the treatment control, a-PD-1 alone, or STING-A alone, the a-PD-1 and STING-A combo significantly increased the $CD11b^-CD103^+$subtype of DCs(Fig.2B), which are known to play a role in the cross-presentation of tumor antigens[20]. TILs from non-target liver metastases showed that the combo treatment resulted in a significant increase in $CD8^+$T cells comparing not only to the treatment control, but also to a-PD-1 alone(Fig.2C). The infiltration of $CD8^+PD\text{-}1^+$T cells in the combo group was comparable with the control group and significantly lower than that in the STING-A alone group(Fig.S1D). Moreover, $CD4^+$T cells and $CD4^+PD\text{-}1^+$T cells were both significantly decreased in the combo treatment group compared to the STING-A treatment group, presumably due to the treatment effect of a-PD-1(Fig.2C). These results suggest that, in non-target liver metastatic lesions, $CD8^+$ and $CD4^+$T cells both trended in the favor of anti-tumor immune response following the a-PD-1

and STING-A combo treatment. In non-target liver metastases, $MHCII^{+}CD11c^{+}$DCs were similar among all treatment groups, suggesting that an enhanced antigen presentation was originated in locally targeted lesions. However, $CD11b^{-}CD103^{+}$DCs were significantly elevated in the combo treatment group in non-target lesions(Fig.2D). It is possible that $CD103^{+}$DCs trafficked from targeted lesions to non-target lesions. Taken together, these results suggest that both STING-A and a-PD-1 are required to activate local immune response in favor of anti-tumor response and that this immune response is extended to the non-target lesions in the vicinity of the target lesion.

STING-A in combination with anti-PD-1 antibody activate anti-tumor immunity via innate immune response signaling pathways

As the flow cytometry analysis has limitation in examining cytokine/chemokines and intracellular signals involved in the innate immune response, we examined the gene regulation of innate immune response following STING-A and/or a-PD-1 treatment by using the NanoString assays with the murine PanCancer Immune panel. We selected differentially expressed genes by comparing the STING-A and a-PD-1 combo treatment and treatment controls, STING-A alone or a-PD-1 alone with a 5% false discovery rate(Fig.S1E). We first examined the gene expression in the interferon(IFN) response pathways. As shown in Fig.2E, the gene expression of IFN-γ (*Ifng*) was significantly increased in the combo treatment group and was also accompanied by significantly increased expression of *Ifngr1*, *Ifnar2*, *Irf1*, *Irf4*, *Irf5*, *Irf7*, *Irf8*, *Stat1*, *Stat2*, *Stat4*, *Ifitm1*, *Ifih1*, *Ifit1*, *Ifit2*, *Ifit3*, *Ifi35*, and *Ifi44* compared to the control or single treatment groups. However, *Irf3* was significantly decreased in the

combo treatment group compared to the a-PD-1 treatment group(Fig.S1F). In addition, the tumor necrosis factor(TNF)-response pathway genes including *Tnf*(encoding TNF-α), *Lta*(encoding TNF-β), *Nfkb1*, *Nfkb2*, and *Tank* were also significantly upregulated in the combo treatment group compared to the control or single treatment groups(Fig.2F). The innate immune response pathways genes including *Tmem173(STING*), *Ddx58*, *Nlrp3*, *Nlrc5*, *Myd88*, *Clec4a2*, *Clec4n*, *Clec5a*, *Clec7a*, *Nod1*, and *Nod2* were significantly increased in the combo treatment group compared to the control or single treatment groups(Fig.2G). However, as anticipated, the gene expression of *Jak1* and *Jak2* was similar among all treatment groups, suggesting *Jak1/2* are not regulated at the RNA level(Fig.S1F).

We next investigated the expression of cytokines which are known to be involved in the development and differentiation of T and B lymphocytes(Fig.3A-B;Fig.S2A-B). As shown in Fig.3A, the expression of most genes in the interleukin(IL)-1 and IL-18 family except *Il18* itself and *Irak1* was significantly increased in the combo treatment group compared to most of other treatment groups. As demonstrated in Fig.3B, the gene expression of most of the proinflammatory cytokine receptors including *Il2ra*, *Il2rb*, *Il2rg*, *Il7r*, *Il12rb1*, *Il12rb2*, *l13ra1*, *Il13ra2*, and *Il15ra* was significantly increased in the combo treatment group compared to most of other treatment groups. Interestingly, the cytokines themselves including *Il2*, *Il7*, *Il12*, and *Il13*, besides *Il21* which was significantly upregulated, were upregulated in a non-statistically significant trend in the combo treatment group compared to the control or single treatment groups(Fig.S2A). These results suggest that pro-inflammatory pathways including those that mediate the inflammasome are activated broadly by the combination of

the STING-A and a-PD-1.

As anticipated, we found that the majority of chemokine genes were upregulated in the combo treatment group compared to the a-PD-1 treatment group(Fig.S2C), likely due to the innate immune response induced by the STING-A. Therefore, we focused on those associated with T cell trafficking. Our results demonstrate a significantly increased expression of *Ccl1*, *Ccl2*, *Ccl3*, *Ccl4*, *Ccl5*, *Ccl7*, and *Ccl8* in the combo treatment group compared to the vehicle control treatment group(Fig.3C), suggesting that stimulation of innate immune response is anticipated to induce myeloid cell infiltration. C-X-C motif chemokine ligand(CXCL) 9, CXCL10, and CXCL11 are known to bind C-X-C motif chemokine receptor(CXCR) 3 on T cells and, in response to IFN signaling to recruit memory and activated effector T cells[21]. We observed a significant enhancement of the expression of *Cxcl9*, *Cxcl10*, and *Cxcl11* in the combo treatment group compared with the control or single treatment groups(Fig.3C) although the expression of *Cxcr3* was similar among different treatment groups(Fig.S1E). Interestingly, comparing to the vehicle control treatment group, the administration of a-PD-1 showed a statistically non-significant trend of increase whereas STING-A showed a trend of decease in the expression of *Ccl17*, which encodes a T regulatory cell(Treg) chemokine. This finding is thus consistent with published studies showing that ICIs upregulate C-C motif chemokine ligand(CCL) 17 expression in tumors and increase the migration of Tregs into the TME of PDAC[22, 23]. Moreover, we here observed that the combo treatment led to a significantly decreased expression of *Ccl17(*Fig.3C;Fig.S2D). It should be noted that the gene expression results from the NanoString assay may be influenced by an influx of immune cells

that express the genes. Therefore, an increased expression of certain immune genes may represent an increased infiltration of the relevant immune subtypes. Taken together, these results suggest that STING-A may confer an antitumor effect by suppressing CCL17 expression or CCL17-expressing cells and thereby suppressing Treg migration into the TME.

STING-A in combination with anti-PD-1 antibody enhances T cell activation signals

Among those differentially expressed genes in the above NanoString analysis, we did further statistical analysis on genes related to the activation of effector T cells. As shown in Fig.S2E and as anticipated, the expression of T cell receptor/CD3 signaling pathway genes including *Cd3d*, *Cd3e*, *Cd3g*, *Cd3z*, *Cd8a*, and *Lck* in the combo treatment group was significantly increased[24, 25]. In addition, our results(Fig.3D) revealed that *Gzma*, *Gzmb*, *Gzmk*, and *Prf1* expression was significantly elevated in the combo treatment group comparing to most of other treatment groups, suggesting that the cytotoxic function of effector T cells are significantly enhanced. The gene expression of T cell co-stimulatory factors including *Tnfrsf9*(CD137), *Tnfrsf4*(OX40), and *Icos* were significantly increased in the combo treatment group when compared to any other group and including *Cd27* when compared to the vehicle treatment group(Fig.3E). However, the gene expression of co-inhibitory receptors including *Pdcd1*(PD-1), *Lag3*, *Havcr2*(TIM3), and *Ctla4* and the expression of immune checkpoint activators such as *Cd274*(PD-L1) and *Ido1* were significantly elevated in the combo treatment group compared to any other treatment group(Fig.3F;Fig.S2F). These results suggested that T cell activation in the combo treatment group may also lead to the T cell exhaustion, in consistence with previously published studies[26].

STING-A in combination with anti-PD-1 antibody enhances the infiltration and activation of effector T cells in the distant subcutaneous tumors

We next examined the immune response that mediates the abscopal effects in the distant tumors. As shown in Fig.4A, we observed a significant increase in the infiltration of $CD8^+$ and $CD8^+PD\text{-}1^+$T cells in the SubQ tumors from the combo treatment group, supporting the abscopal effect. Similar to the locally targeted lesions, $CD4^+$ and $CD4^+PD\text{-}1^+$T cells in the SubQ tumors were not significantly changed among all treatment groups. $CD11b^-CD103^+$DCs in the SubQ tumors were also similar among all treatment groups, suggesting that the activation of antigen presenting cells occurred locally(Fig.4B).

We then used the same NanoString assay to assess the T cell functional status. The results indicate that the expression of genes associated with the T-cell receptor CD3 complex exhibited a similarly significant increase in the SubQ tumors from the combo treatment group compared to other treatment groups as in the liver metastases(Fig.S3A). Similarly, genes related to the cytotoxic activities of effector T cells, including *Gzma*, *Gzmb*, *Gzmk*, and *Prf1*, demonstrated a significant increase in the combo treatment group compared to most of other treatment groups(Fig.4C). In addition, the combo treatment group exhibited a significant increase in the expression of signals related to T cell activation including *Cd27*, *Icos*, *Cd274*(PD-L1), and *Ido1* comparing to most of other treatment groups(Fig.4D-E) and including *Cd28*, *Cd80*, *Pdcd1*(PD-1), *Lag3*, and *Ctla4* comparing to the vehicle treatment group(Fig.S3B). Consistently, genes related to chemokines for effector T cell trafficking

including *Cxcl9*, *Cxcl10*, and *Cxcl11* exhibited a significant increase in their expression in the combo treatment group compared to most of other treatment groups(Fig.4F). *Ccl17* also exhibited a significant decrease in the combo treatment group compared to the vehicle treatment group. Interestingly, the expression of *Ccl28*, a T and B cell homing factor[27], showed a significant increase in the combo treatment group in SubQ tumors(Fig.4F), but not the target metastatic lesions(Fig.S2C). The gene expression of cytokines and cytokine receptors that are relevant to the activated status of T cells was similarly increased as seen in the liver metastases, again except *Il18*(Fig.4F), further supporting the abscopal effect.

In addition, the profiles of other cytokines and chemokines in the SubQ tumors were similar to those in the targeted liver metastases and showed a significant increase in pro-inflammatory immune responses in the IFN(Fig.4G) and TNF pathways(Fig.4H), but no significant changes or a decrease in *Jak1* and *Jak2*(Fig.S3C), in the combo treatment group compared to other treatment groups. Nevertheless, expression of innate agonist receptors and adaptors in SubQ tumors appeared to be somewhat different from that in targeted liver metastases, showing an increase in *Tlr8*, *Nlrc5*, *Nlrp3*, *Clec4n*, *Clec5a*, *Clec7a*, and *Nod1*, but a decrease in *Ticam1* and *Mavs* in the combo treatment group compared to other treatment groups(Fig.4I). However, the profile of chemokines and chemokine receptors that function in the myeloid cell trafficking was similar between targeted liver metastases and distant SubQ tumors in the combo treatment group compared to other treatment groups(Fig.S3D).

Establish a mouse model for systemic administration of STING-A in combination with

anti-PD-1 antibody induced both systemic and intratumoral immune responses

We next tested the IM administration, a systemic administrative route, of STING-A. To compare the anti-tumor efficacy of IM with IT injection of STING-A, we used the same liver metastasis model with implantation of SubQ tumors by following the same schema described in Fig.1B. Firstly, systemic administration did not show any obvious toxicity including bleeding, unhealed wound, paralysis, or weight loss, etc. All the mice following the hemisplenectomy procedure were candidates for IM injection although we chose those feasible for IT injection for the purpose of comparison. We then found that mice in the combo(IM) group had a significantly prolonged survival when compared to other treatment groups(Fig.5A). The TGI rate for SubQ tumors also exhibited a significant increase in the combo(IM) group(maximum TGI=58.86 ± 49.12%, $p < 0.05$)(Fig.5B). By combining the survival data in both IT and IM experiments, we found that the majority of mice died at around 3 to 4 weeks after tumor implantation whereas those who received both STING-A by IT or IM and a-PD-1 may live up to 6 weeks(Fig.S4A). Mice who received STING-A intramuscularly in combination with a-PD-1 reached the longest survival beyond 6 weeks although, likely due to the small sample size, there was no significant survival difference between the IM combo and the IT combo group.

To assess the systemic immune response induced by the IM injection of STING-A and/or a-PD-1, we first measured the cytokine response in the serum samples harvested 6 hours after the IM injection of STING-A. The results demonstrated that a number of cytokines especially those associated with inflammation had a significantly increased level in the sera of mice

392 from the combo treatment group, including TNF-α, and IFN-γ(Fig.5C). Interestingly, several
393 T lymphocytes trafficking chemokines including CXCL9, and CXCL10 and type I cytokines
394 including IL-2[28] and IL-12[29] were significantly increased in the sera from mice in the
395 combo treatment group compared to other treatment groups, suggesting that IM injection of
396 STING-A in combination with a-PD-1 is potentially able to induce an anti-tumor systemic
397 immune response(Fig.5D). In addition, some interleukins including IL-5[30], IL-6[31], and
398 IL-10[32] that support lymphocyte growth and/or antibody production were also boosted in
399 the IM combo group(Fig.S4B). The results also indicated the increased production of
400 cytokines that participate in the recruitment of macrophages, neutrophils, and eosinophils,
401 including CCL2, CCL3, CCL4, CCL5, CXCL1, granulocyte colony stimulating factor(G-
402 CSF), and CCL11(Fig.S4C). These results suggested that the IM injection of STING-A is
403 able to induce similar systemic immune responses as evidenced by the above described
404 Nanostring analysis following the IT injection of STING-A.
405
406 Next, we assessed TILs by dissecting a single target liver metastatic lesion and a mixture of
407 non-target liver metastases, respectively, in this model treated by IM injection of STING-A.
408 The single target liver lesion was pre-selected as it would be selected for the IT treatment, but
409 without any IT treatment to be given(Fig.5E-H;Fig.S4D-E). As shown in Fig.5E-F, IM
410 injection of STING-A alone significantly enhanced the infiltration of $CD8^+$ and $CD4^+$T cells
411 in both the pre-selected liver metastatic lesion and other liver metastases. The enhancement
412 of the T cell infiltration was not as high in the IM combo group as the IM STING-A alone
413 group. Nevertheless, $CD103^+$DCs showed a similar profile in the tumors with the IM

injection of STING-A(Fig.5G-H) compared to those shown above with the IT injection of STING-A, suggesting that systemic IM injection of STING-A is able to activate the desired antigen-presenting process in the liver metastases.

We then performed the NanoString analyses of liver metastases and SubQ tumors and compared them among treatment groups. As shown in the Fig.S5A, the high-throughput analysis of the NanoString results only revealed a smaller number of genes that were differentially expressed among the treatment groups than those differentially expressed among the treatment groups with the IT injection of STING-A(Fig.S1E). The results however supported a non-significant increasing trend in the expression of genes associated with the IFN response pathways in the liver metastases in the IM combo group(Fig.S5B). Nevertheless, in the STING-A IM alone treatment group, the expression of T cell co-stimulatory molecules including *Tnfrsf4(*OX40), *Cd27*, *Tnfrsf9*(CD137), and *Icos* exhibited a trend(Fig.S5C) consistent with the results in the single STING-A IT treatment group(Fig.3E). However, the IM injection of STING-A combined with a-PD-1 did not significantly increase the expression of these co-stimulatory molecules, together with the above T cell infiltration results(Fig.5E-F), suggesting a-PD-1 or a-PD-1 alone may not be an optimal immune checkpoint inhibitor treatment strategy in combination with STING-A. Nevertheless, we observed a strong trend of increased expression of genes related to the cytotoxic activities of effector T cells in the IM combo group including *Gzma*, *Gzmb*, *Gzmk*, and *Prf1*(Fig.S5D). Chemokines especially those involved in effector T cell trafficking including *Cxcl9*, *Cxcl10*, and *Cxcl11* exhibited similar trend as those genes associated with cytotoxic activities of

effector T cells(Fig.S5E). In contrast, the increase in the T cell exhaustion and immune checkpoint signals and myeloid cell-recruiting cytokine/chemokine signals that were observed with the IT combo treatment were not observed in the IM combo group(Fig.6A).

We also examined the immune response in the SubQ tumors in the experiment with the IM injection of STING-A. As shown in Fig.S6A, we observed a significant decrease in the infiltration ratio of $CD4^{+}PD\text{-}1^{+}$T cells in the $CD4^{+}$T cells in the SubQ tumors from the IM combo treatment group. A similar decreasing trend of $CD8^{+}PD\text{-}1^{+}$T cells was observed(Fig.S6A), demonstrating the treatment effect of a-PD-1. Next, we used the same NanoString assays to assess the T cell functional status within the SubQ tumors. Interestingly, unlike the results in the liver metastases, the expression of genes associated with the T-cell receptor CD3 complex exhibited a significant increase(*Cd3z*) or a strong increasing trend in the SubQ tumors from the combo treatment group compared to other treatment groups(Fig.S6B). T cell co-stimulatory molecules including *Tnfrsf4(*OX40), *Tnfrsf9*(CD137), *Cd80*, and *Icos* all exhibited an increasing trend(Fig.S6C). In addition, the IM combo treatment group exhibited a significantly increased expression of *Il7r*(Fig.S6D), which has been shown to play a critical role in the development of lymphocytes in the process known as V(D)J recombination[33]. These results suggest that there may be an intertumoral heterogeneity in the immune response to the systemic administration of STING-A. However, we found that the T cell exhaustion and immune checkpoint signals exhibited an enhanced expression in the IM combo treatment group compared to other treatment groups(Fig.6B). These results suggest that an enhanced T cell activation status and cytotoxic function in

response to either IT or IM treatment of STING-A is associated with upregulation of T cell exhaustion signals and CTLA-4.

The overall increasing trend of those chemokines/chemokine receptors involved in the myeloid cell recruitment was less significant in both liver metastases(Fig.S5E) and SubQ tumors(Fig.S6D) than that in the IT combo group, suggesting that systemic delivery of STING-A does not lead to a strong induction of immunosuppressive signals. It is noteworthy to mention that *Ccr5* expression in the SubQ tumors was significantly reduced by the treatment of a-PD-1 compared to the vehicle treatment group, but was significantly enhanced following the IM injection of STING-A in combination with a-PD-1(Fig.S6E). This result appears to be in consistent with the agonistic effect of C-C motif chemokine receptor(CCR) 5 expression previously reported in the PDAC models[34].

In addition to above differences between tumors from IM treated groups and IT treated groups, we noted that the expression of immunosuppressive myeloid cells associated-genes including *Apoe*, *Trem2*, *Cxcr4*, and *Abcg1* was significantly increased in the SubQ tumors from the IM combo treatment group, but not the SubQ tumors from the IT combo treatment group, compared to the respective control group(Fig.6C-F). Such a difference was not observed in the comparison between liver metastases from the IM combo treatment group and the IT combo treatment group(Fig.S6F-I). These results suggest that systemic administration of STING-A could still induce certain immunosuppressive signals that require additional targeted treatments.

STING-A in combination with immune checkpoint inhibitors significantly improved the survival of genetically engineered KPC mice that develops invasive PDAC spontaneously.

Thus, above results suggest that systemic IM administration of STING-A led to less induction of immunosuppressive signals while maintaining a systemic and intratumoral immune response that favors antitumor response. These results also provide the mechanistic basis of the enhanced anti-tumor activity of the IM STING-A observed in the implanted tumor model(Fig.5). We next validated this antitumor activity in the genetically engineered KPC mice that develops invasive PDAC spontaneously in a manner resembling human PDAC pathogenesis. As CTLA-4 remains to be one of immunosuppressive signals presented in the tumors treated by IM STING-A, we included anti-CTLA4 antibody to the immune checkpoint inhibitor regimen. KPC mice were subjected to weekly to twice weekly ultrasonic screening at age of 3 months and enrolled in the experiment once either the length, width, or height of the pancreatic tumor reached 2.00 mm to ensure eligible mice had equivalent tumor burdens. As shown in Fig.7A, eligible KPC mice were randomized into the three treatment groups to receive a total of seven injections. Treatment toxicity and mouse survival were monitored for 3 months following the first treatment. No treatment related toxicity including local toxicity related to IM injection sites was observed. The STING-A monotherapy did not show any antitumor activity in a later experiment(manuscript in preparation). Dual checkpoint inhibitors failed to improve the overall survival of KPC mice when compared with control group; however, the co-administration of IM STING-A with dual checkpoint

inhibitors significantly prolonged the survival of the KPC mice(Fig.7B).

Systemic administration and intratumoral administration of an NLRP3 agonist in combination with anti-PD-1 antibody has a similar efficacy

In this study, we attempted to understand whether systemic administration can be applied to another innate immune agonist. We found that the combination of IT injection of NACHT, LRR, and PYD domains-containing protein 3(NLRP3) agonist and a-PD-1 had similar anti-tumor efficacy as the combination of IT injection of STING-A and a-PD-1 and prolonged the survival of liver metastasis mice implanted with SubQ tumors as compared to a-PD-1 alone, NLRP3 agonist alone, or vehicle control(Fig.S7A). Likely due to the small sample size, the combination of NLRP3 agonist and a-PD-1 failed to induce a significantly stronger tumor growth inhibition on either liver metastatic lesion or the SubQ tumors than single treatment groups(Fig.S7B-C). However, different routes of administration of NLRP3 agonist including IT, tail-vein injection, or intra-subcutaneous tumor injection resulted in no survival difference of the liver metastasis mice(Fig.S7D). Despite a small sample size, NanoString analysis showed that the expression of *Gzmk*(Fig.S7E), an effector T cell cytotoxicity-associated gene, was significantly increased in the NLRP3 agonist-treated tumor, but not in the STING-A-treated tumor(Fig.3D), suggesting that further investigation of systemic administration of other innate immune agonists such as NLRP3 agonist is warranted.

Discussion

To our knowledge, this study is one of the few exploring the effects of the STING-A in

combination with ICIs for the treatment of PDAC in a pancreatic liver metastasis murine model. We previously used this mouse model to support the application of STING-A as an adjuvant for the vaccine therapy. This mouse model resembles the spontaneous development of liver metastases in human PDACs and has been used in multiple prior studies for the preclinical development of rationale immunotherapy combinations[35, 36, 37]. The TME of the liver metastases in this model is similar to that of orthotopically implanted KPC tumors[38]. Our study demonstrated the antitumor efficacy of the combinational treatment with STING-A and PD-1 blockade in this liver metastasis model as well as novel evidence that demonstrated the survival benefit of the combination of a STING-A and ICIs in the genetically engineered, spontaneously formed KPC tumor model. In our model, STING-A in combination with a-PD-1 enhances effector T cells infiltration and $CD103^{+}$dendritic cells in both target liver metastatic lesions and non-target metastatic lesions as well as distant tumor lesions that are resembled by subQ tumors. More importantly, this study demonstrated that systemic administration of STING-A is equivalent to the intratumoral injection in both antitumor efficacy and immune response. Neither systemic nor intratumoral administration resulted in obvious toxicities; however, systemic administration was more feasible than intratumoral administration and also avoided any intragenic liver injury. Our study also supported the feasibility of administrating an NLRP3 agonist systemically and would supports a new paradigm of the clinical development of innate immune agonists by systemic administration.

Our results suggest that IM injection of STING-A is able to induce similar systemic immune

responses as the IT injection of STING-A. Systemic IM injection of STING-A is also able to activate the desired antigen-presenting process in the liver metastases. Although the effector T cell responses appear to be slightly weaker in the IM injection of STING-A, the increase in the T cell exhaustion and immune checkpoint signals and myeloid cell-recruiting cytokine/chemokine signals that were observed with the IT combo treatment were not observed in the IM combo group.

Although this study did not demonstrate a significant difference in the treatment response between IM and IT injections of STING-A, we observed that mice who received IM injections of STING-A in combination with a-PD-1 survived longer than 6 weeks whereas none of the mice who received IT injection of STING-A in combination with a-PD-1 survived longer than 6 weeks. Therefore, it might be possible to see the survival benefit of the IM injection of STING-A if the sample size would potentially be larger; however, the sample size in each experiment was limited by the technical difficulty of IT injection. As it would be a challenge to breed a large number of the KPC transgenic mice for being randomized to multiple treatment groups, we decided to test the combination of a-PD-1 and anti-CTLA-4 antibody instead of two ICIs by itself in the experiments with the KPC transgenic mice. Our results suggest that an enhanced T cell activation status and cytotoxic function in response to either IT or IM treatment of STING-A is associated with CTLA-4 upregulation. Hence, the reason we included anti-CTLA-4 antibody to a-PD-1 in the experiment with the KPC transgenic mice. Future studies could compare the combination of a-PD-1 and anti-CTLA-4 antibody with either a-PD-1 alone or anti-CTLA-4 antibody alone.

This study has a few limitations, first being the smaller sample size. As discussed above, the sample size is limited by the technical complexity of IT injection and breeding KPC transgenic mice. However, the sample size in the current study is, to our knowledge the largest one in testing the intratumor injection of the tumors in internal organs. It is also one of the largest using the KPC transgenic mice as the preclinical model for the efficacy testing. However, the current sample size allowed this study to repeat most of the experiments. Second, this study did not examine the effect of anti-CTL4-4 antibody separately from the treatment groups testing the combination of a-PD-1 and anti-CTLA-4 antibody. Third, chemotherapy, as a current standard of care treatment, was not included in the experiments in this study. We were concerned that chemotherapy would complicate our comparison of the antitumor efficacy and immune response between the IM and IT injection of STING-A. We are studying the combination of chemotherapy and STING-A in an independent study.

To test the feasibility of systemic administration of other innate immune agonists, we examined the NLRP3 agonist in this study. Although it may have been limited by the small sample size, this study demonstrated that there were no significant differences in anti-tumor efficacy between intratumoral and systemic administration of NLRP3 agonist. This study has not performed an in-depth investigation on the NLRP3 agonist. However, with limited data, this study suggests that further investigation of systemic administration of other innate immune agonists such as NLRP3 agonist is warranted. The results in this study have thus supported the phase 1 trial that evaluated BMS-986301 intratumoral or intravenous injection

as monotherapy or in combination with nivolumab(PD-1 blockade) and ipilimumab in patients with advanced solid cancers(NCT03956680).

Abbreviations: PDAC, pancreatic ductal adenocarcinoma; TME, tumor microenvironment; STING, stimulator of interferon genes; PD-1, programmed cell death protein 1; CTLA-4, cytotoxic T-lymphocyte associated protein 4; KPC, Kras/p53/pdx1-Cre; NLRP3, NACHT, LRR, and PYD domains-containing protein 3; TBK1, TANK-binding kinase 1; IRF3, interferon regulatory factor 3; IFN, interferon; CDN, cyclic dinucleotide; ICI, immune checkpoint inhibitors; TGI, tumor growth inhibition; TIL, tumor infiltrating leucocyte; DC, dendritic cell; IL, interleukin; CXCL, C-X-C motif chemokine ligand; CXCR, C-X-C motif chemokine receptor; CCL, C-C motif chemokine ligand; G-CSF, granulocyte colony stimulating factor ; CCR, C-C motif chemokine receptor.

Declarations

Ethics approval and consent to participate

All studies and maintenance of mice were conducted in accordance with the approval of the Institutional Animal Care and Use Committee (IACUC) guidelines of Johns Hopkins School of Medicine (Animal Protocol: MO22M59).

Consent for publication

Not applicable.

Availability of data and materials

All data needed to evaluate the conclusions in the paper are present in the paper and the Supplementary Materials. Any further information required to support our data will be supplied upon request.

Competing interests

L.Z. receives grant support from Bristol-Meyer Squibb, Merck, AstraZeneca, iTeos, Amgen, NovaRock, Inxmed, Halozyme and Abmeta. L.Z. is a paid consultant/Advisory Board Member at Biosion, Alphamab, NovaRock, Ambrx, Akrevia/Xilio, QED, Novagenesis, Snow Lake Capitals, Amberstone, Pfizer, Tavotek, and Mingruizhiyao. L.Z. holds shares at Alphamab, Amberstone, Mingruizhiyao, and Cellaration.

Funding

This study was supported by a Bristol-Myers Squibb II-ON grant (L. Zheng). LZ is supported by an NIH Grant R01 CA169702, an NIH Grant R01 CA197296, an NIH Grant P01 CA247886, an NIH SPORE Grant P50 CA062924, and an NIH Cancer Center Support Grant P30 CA006973. KL is supported by a National Natural Science Foundation of China 82303740, a Key Research and Development Project of Science and Technology Department of Sichuan Province 2023YFS0167, a China Postdoctoral Science Foundation 2023T160451, and a West China Hospital Postdoctoral Science Foundation 2023HXBH053.

Authors' contributions

Keyu Li and Junke Wang contributed equally to this project. Concept was conceived by L.Z. The strategy and the overall study were designed by K.L. and L.Z. Experiments were conducted by K.L., Junke W., N.N., N.J., A.B., Jiangxin W., M.H., J.Y., D.T., B.E., C.Y., and M. W. Data were collected by K.L. and Junke W. Formal analysis was conducted by K.L., Junke W, and Y.X. Genetically modified mice were generated by M.H, V.F., and M.L. Original draft manuscript was written by K.L. Manuscript was reviewed and revised was by A.O., B.E., M.W., and L.Z. Supervision was made by X.L., Y.W., and L.Z. The project administrator is L.Z.

Acknowledgments

We would like to acknowledge the important insight provided by Jie Fang, Gary Schieven, and Jordan Blum from the Bristol-Myers Squibb group. This work was done at the Johns Hopkins University.

References

1 Demaria O, Cornen S, Daëron M, Morel Y, Medzhitov R, Vivier E. Harnessing innate immunity in cancer therapy. Nature 2019;**574**:45-56.

2 Rameshbabu S, Labadie BW, Argulian A, Patnaik A. Targeting innate immunity in cancer therapy. Vaccines 2021;**9**:138.

3 Mohseni G, Li J, Ariston Gabriel AN, Du L, Wang Y-s, Wang C. The function of cGAS-STING pathway in treatment of pancreatic cancer. Front Immunol 2021;**12**:781032.

4 Barber GN. STING: infection, inflammation and cancer. Nature Reviews Immunology

2015;**15**:760.

5 Zhang T, Ma C, Zhang Z, Zhang H, Hu H. NF-κB signaling in inflammation and cancer. MedComm 2021;**2**:618-53.

6 Kwon J, Bakhoum SF. The cytosolic DNA-sensing cGAS–STING pathway in cancer. Cancer discovery 2020;**10**:26-39.

7 Ni H, Zhang H, Li L, Huang H, Guo H, Zhang L*, et al.* T cell-intrinsic STING signaling promotes regulatory T cell induction and immunosuppression by upregulating FOXP3 transcription in cervical cancer. Journal for Immunotherapy of Cancer 2022;**10**.

8 Amouzegar A, Chelvanambi M, Filderman JN, Storkus WJ, Luke JJ. STING agonists as cancer therapeutics. Cancers (Basel) 2021;**13**:2695.

9 Le Naour J, Zitvogel L, Galluzzi L, Vacchelli E, Kroemer G. Trial watch: STING agonists in cancer therapy. Oncoimmunology 2020;**9**:1777624.

10 Ding C, Song Z, Shen A, Chen T, Zhang A. Small molecules targeting the innate immune cGAS–STING–TBK1 signaling pathway. Acta Pharmaceutica Sinica B 2020;**10**:2272-98.

11 Clark CE, Beatty GL, Vonderheide RH. Immunosurveillance of pancreatic adenocarcinoma: insights from genetically engineered mouse models of cancer. Cancer Lett 2009;**279**:1-7.

12 Koido S, Homma S, Takahara A, Namiki Y, Tsukinaga S, Mitobe J*, et al.* Current immunotherapeutic approaches in pancreatic cancer. Clin Dev Immunol 2011;**2011**:267539.

13 Jing W, McAllister D, Vonderhaar EP, Palen K, Riese MJ, Gershan J*, et al.* STING agonist inflames the pancreatic cancer immune microenvironment and reduces tumor burden in mouse models. Journal for immunotherapy of cancer 2019;**7**:115.

14 Schieven G, Brown J, Swanson J, Stromko B, Ho C, Zhang R*, et al.* Preclinical characterization

678 of BMS-986301, a differentiated STING agonist with robust antitumor activity as monotherapy or in
679 combination with anti-PD-1. Proceedings of the 33rd Annual Meeting & Pre-Conference Programs of
680 the Society for Immunotherapy of Cancer (SITC 2018), Washington, DC, USA, 2018:7-11.
681 15 Vonderhaar EP, Barnekow NS, McAllister D, McOlash L, Eid MA, Riese MJ, *et al.* STING
682 activated tumor-intrinsic type I interferon signaling promotes CXCR3 dependent antitumor immunity in
683 pancreatic cancer. Cellular and molecular gastroenterology and hepatology 2021;**12**:41-58.
684 16 Hingorani SR, Wang L, Multani AS, Combs C, Deramaudt TB, Hruban RH, *et al.* Trp53R172H
685 and KrasG12D cooperate to promote chromosomal instability and widely metastatic pancreatic ductal
686 adenocarcinoma in mice. Cancer cell 2005;**7**:469-83.
687 17 Soares KC, Foley K, Olino K, Leubner A, Mayo SC, Jain A, *et al.* A preclinical murine model of
688 hepatic metastases. J Vis Exp 2014:51677.
689 18 Blair AB, Kleponis J, Thomas DL, 2nd, Muth ST, Murphy AG, Kim V, *et al.* IDO1 inhibition
690 potentiates vaccine-induced immunity against pancreatic adenocarcinoma. J Clin Invest
691 2019;**129**:1742-55.
692 19 Tang H, Panemangalore R, Yarde M, Zhang L, Cvijic ME. 384-well multiplexed luminex cytokine
693 assays for lead optimization. Journal of biomolecular screening 2016;**21**:548-55.
694 20 Joffre OP, Segura E, Savina A, Amigorena S. Cross-presentation by dendritic cells. Nature
695 Reviews Immunology 2012;**12**:557-69.
696 21 Tokunaga R, Zhang W, Naseem M, Puccini A, Berger MD, Soni S, *et al.* CXCL9, CXCL10,
697 CXCL11/CXCR3 axis for immune activation–a target for novel cancer therapy. Cancer treatment
698 reviews 2018;**63**:40-7.
699 22 Mizukami Y, Kono K, Kawaguchi Y, Akaike H, Kamimura K, Sugai H, *et al.* CCL17 and CCL22

700 chemokines within tumor microenvironment are related to accumulation of Foxp3+regulatory T cells in
701 gastric cancer. Int J Cancer 2008;**122**:2286-93.
702 23 Marshall LA, Marubayashi S, Jorapur A, Jacobson S, Zibinsky M, Robles O*, et al.* Tumors
703 establish resistance to immunotherapy by regulating Treg recruitment via CCR4. Journal for
704 immunotherapy of cancer 2020;**8**.
705 24 Guy CS, Vignali KM, Temirov J, Bettini ML, Overacre AE, Smeltzer M*, et al.* Distinct TCR
706 signaling pathways drive proliferation and cytokine production in T cells. Nat Immunol 2013;**14**:262-70.
707 25 Lipp AM, Juhasz K, Paar C, Ogris C, Eckerstorfer P, Thuenauer R*, et al.* Lck mediates signal
708 transmission from CD59 to the TCR/CD3 pathway in Jurkat T cells. PLoS One 2014;**9**:e85934.
709 26 Wherry EJ, Kurachi M. Molecular and cellular insights into T cell exhaustion. Nature Reviews
710 Immunology 2015;**15**:486-99.
711 27 Mohan T, Deng L, Wang B-Z. CCL28 chemokine: an anchoring point bridging innate and
712 adaptive immunity. Int Immunopharmacol 2017;**51**:165-70.
713 28 Ross SH, Cantrell DA. Signaling and function of interleukin-2 in T lymphocytes. Annu Rev
714 Immunol 2018;**36**:411.
715 29 Gately MK, Wolitzky AG, Quinn PM, Chizzonite R. Regulation of human cytolytic lymphocyte
716 responses by interleukin-12. Cell Immunol 1992;**143**:127-42.
717 30 Molfino N, Gossage D, Kolbeck R, Parker J, Geba G. Molecular and clinical rationale for
718 therapeutic targeting of interleukin-5 and its receptor. Clin Exp Allergy 2012;**42**:712-37.
719 31 Hirano T. IL-6 in inflammation, autoimmunity and cancer. Int Immunol 2021;**33**:127-48.
720 32 Wei H, Li B, Sun A, Guo F. Interleukin-10 family cytokines immunobiology and structure.
721 Structural Immunology 2019:79-96.

722 33 Baizan-Edge A, Stubbs BA, Stubbington MJ, Bolland DJ, Tabbada K, Andrews S*, et al.* IL-7R
723 signaling activates widespread VH and DH gene usage to drive antibody diversity in bone marrow B
724 cells. Cell Reports 2021;**36**:109349.
725 34 Wang J, Saung MT, Li K, Fu J, Fujiwara K, Niu N*, et al.* CCR2/CCR5 inhibitor permits the
726 radiation-induced effector T cell infiltration in pancreatic adenocarcinoma. J Exp Med
727 2022;**219**:e20211631.
728 35 Kim VM, Blair AB, Lauer P, Foley K, Che X, Soares K*, et al.* Anti-pancreatic tumor efficacy of a
729 Listeria-based, Annexin A2-targeting immunotherapy in combination with anti-PD-1 antibodies.
730 Journal for immunotherapy of cancer 2019;**7**:132.
731 36 Muth ST, Saung MT, Blair AB, Henderson MG, Thomas DL, 2nd, Zheng L. CD137 agonist-based
732 combination immunotherapy enhances activated, effector memory T cells and prolongs survival in
733 pancreatic adenocarcinoma. Cancer Lett 2020.
734 37 Blair AB, Wang J, Davelaar J, Baker A, Li K, Niu N*, et al.* Dual stromal targeting sensitizes
735 pancreatic adenocarcinoma for anti-programmed cell death protein 1 therapy. Gastroenterology
736 2022;**163**:1267-80. e7.
737 38 He M, Henderson M, Muth S, Murphy A, Zheng L. Preclinical mouse models for
738 immunotherapeutic and non-immunotherapeutic drug development for pancreatic ductal
739 adenocarcinoma. Ann Pancreat Cancer 2020;**3**.
740
741

Figures and Figure legends

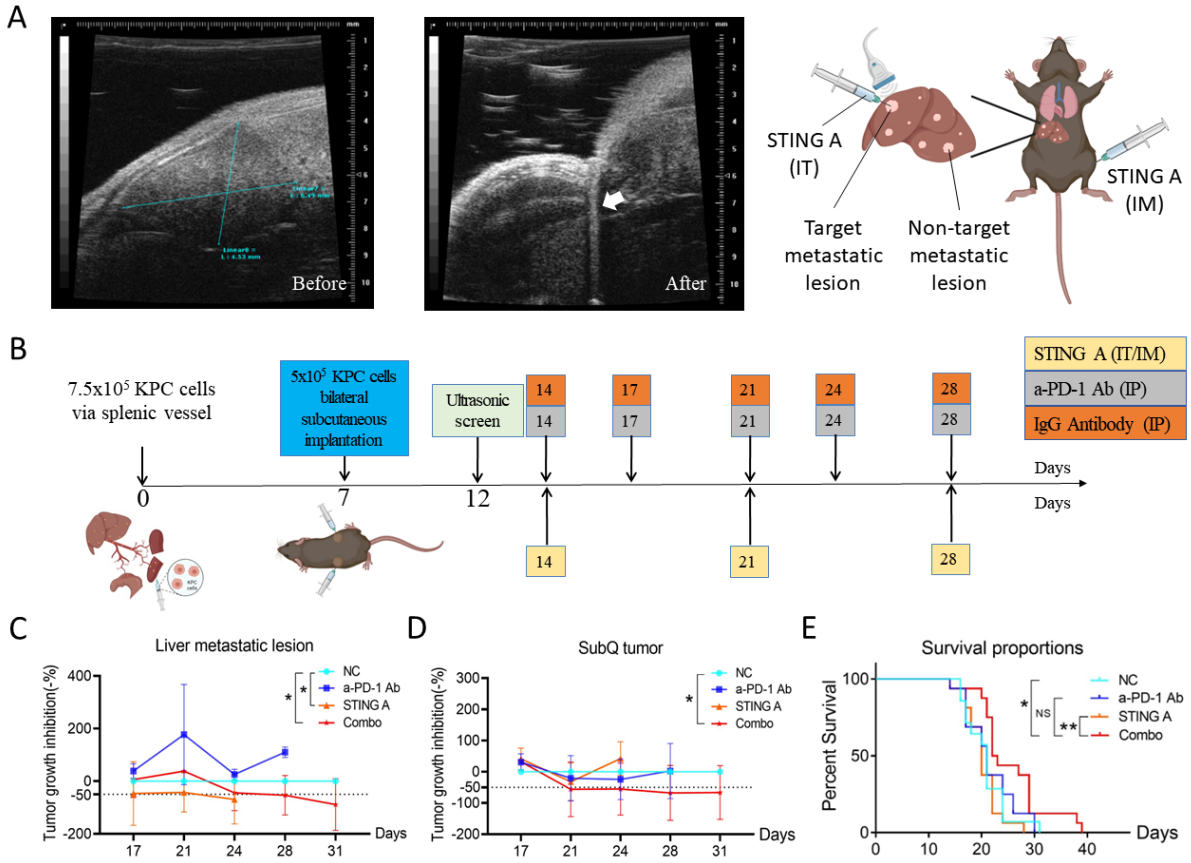

Figure 1. Intratumoral injection of the STING agonist in combination with anti-PD-1 antibody enhance local anti-tumor efficacy with abscopal effects. (A) Ultrasonographic measurement for the target liver metastatic lesion before and after intratumoral injection of the STING agonist. Arrow indicates the injection needle path. (B) Treatment schema. Mice that met inclusion criteria were randomly assigned to each group on day 12 and monitored twice a week until survival endpoints were met. (C) Tumor Growth Inhibition (TGI) of the injected liver metastatic lesion during the treatment period. (D) Tumor Growth Inhibition of the remote subcutaneous (SubQ) tumor during the treatment period. Dashed line at -50% indicates statistically significant TGI. (E) Kaplan-Meier survival curves compare different treatment groups. NC, vehicle/isotype antibody control; STING A, STING agonist; a-PD-1 Ab, anti-PD-1 antibody; Combo, STING A+a-PD-1 Ab; IT, intratumoral; IM, intramuscular; IP, intra-peritoneal. Data shown as mean ± SD; comparison by unpaired t test in C and D, and by Log-rank test in E; *p < 0.05; **p < 0.01; NS, not significant.

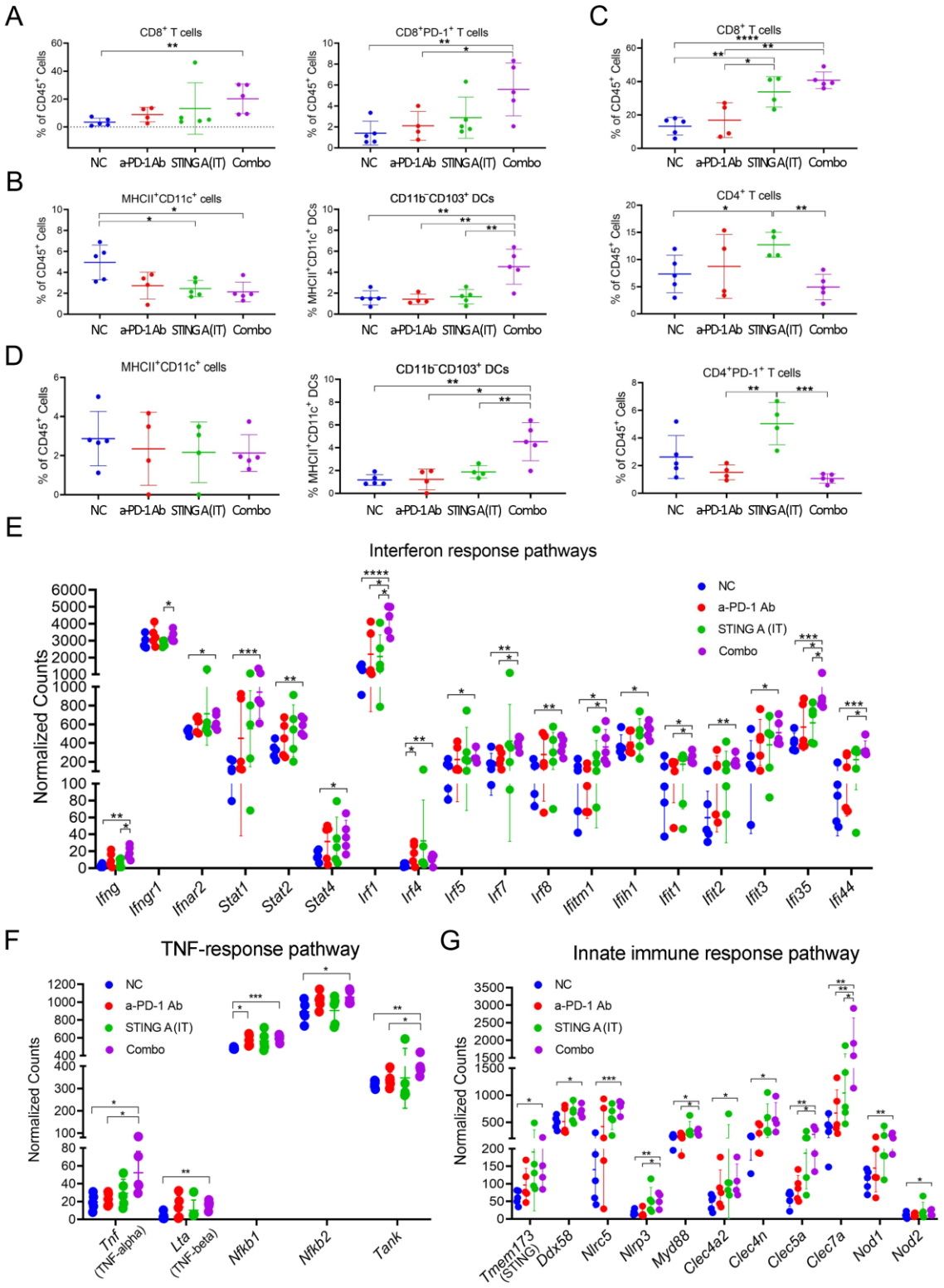
A
CD8+ T cells
CD8+PD-1+ T cells
C
CD8+ T cells
B
MHCII+CD11c+ cells
CD11b-CD103+ DCs
CD4+ T cells
D
MHCII+CD11c+ cells
CD11b-CD103+ DCs
CD4+PD-1+ T cells
% of CD45+ Cells
% MHCII+CD11c+ DCs
NC
a-PD-1Ab
STINGA(IT)
Combo
E
Interferon response pathways
Normalized Counts
NC
a-PD-1 Ab
STING A (IT)
Combo
Ifng
Ifngr1
Ifnar2
Stat1
Stat2
Stat4
Irf1
Irf4
Irf5
Irf7
Irf8
Ifitm1
Ifih1
Ifit1
Ifit2
Ifit3
Ifi35
Ifi44
F
TNF-response pathway
Tnf (TNF-alpha)
Lta (TNF-beta)
Nfkb1
Nfkb2
Tank
G
Innate immune response pathway
Tmem173 (STING)
Ddx58
Nlrc5
Nlrp3
Myd88
Clec4a2
Clec4n
Clec5a
Clec7a
Nod1
Nod2

Figure 2. STING agonist in combination with anti-PD-1 antibody enhances effector T cells and $CD103^+$dendritic cell (DC) infiltration and activates anti-tumor immunity via innate immune response signaling pathways. (A) Percentages of the $CD8^+$ and $CD8^+PD\text{-}1^+$T cells among $CD45^+$leucocytes in the target liver metastatic lesion. (B) Percentages of the $MHCII^+CD11c^+$DC among $CD45^+$leucocytes and the percent of $CD11b^-CD103^+$DC subtype in the target liver metastatic lesion. (C) Percentages of the $CD8^+$, $CD4^+$, and $CD4^+PD\text{-}1^+$T cells among $CD45^+$leucocytes in the non-target liver metastases. (D) Percentages of $MHCII^+CD11c^+$DC among $CD45^+$leucocytes and the percent of $CD11b^-CD103^+$DC subtype in the non-target liver metastases. (E) Expression of genes in the IFN-response pathways in the target liver metastatic lesions from different treatment groups. (F) Expression of genes in the TNF-response pathways in the target liver metastatic lesions from different treatment groups. (G) Expression of genes in the innate immune response pathways in the target liver metastatic lesions from different treatment groups. Data are shown as the mean ± SD; comparison by unpaired t test; *$p < 0.05$; **$p < 0.01$; ***$p < 0.001$; ****$p < 0.0001$. Remaining comparisons are non-significant.

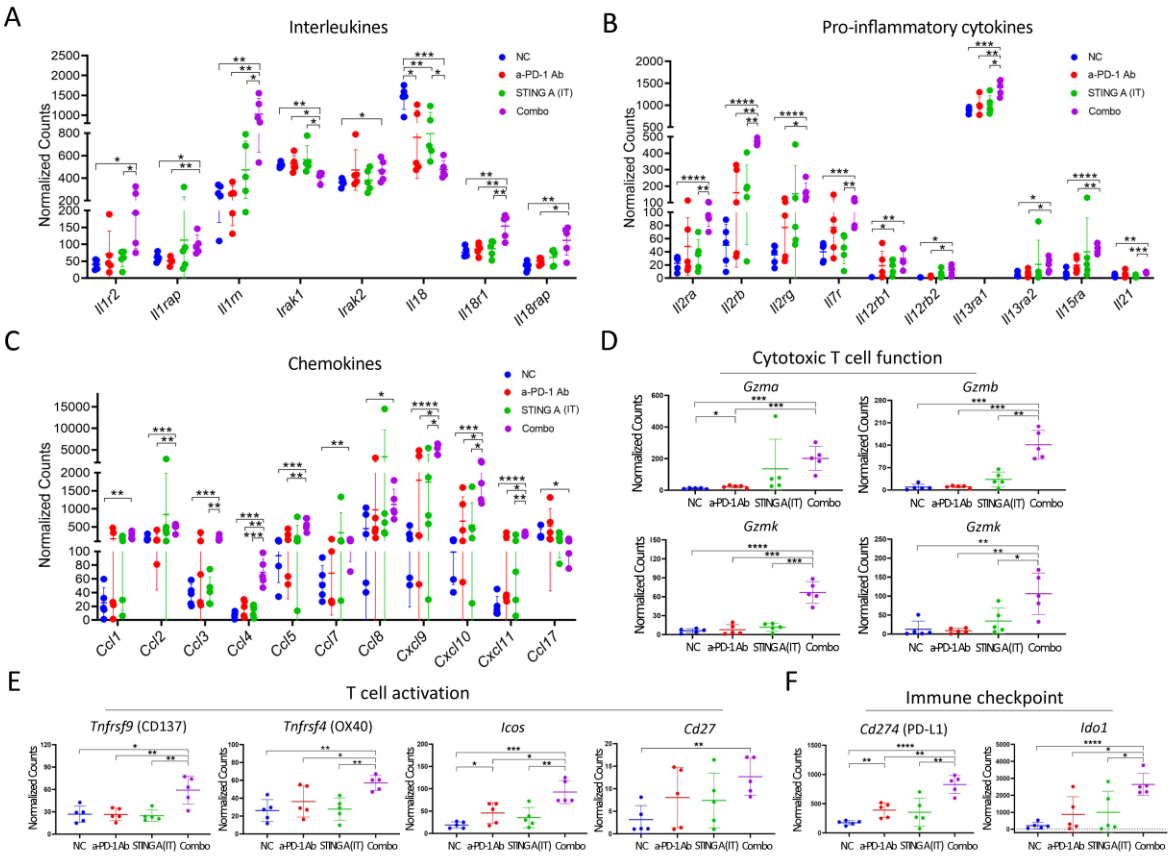

Figure 3. Differentially expressed genes in the target liver metastatic lesions between treatment groups. Expression of genes, as indicated, in the gene families of cytokines (A-B), chemokines (C), the activation of effector T cells (D), the T cell co-stimulatory factors (E), and the immune checkpoint activators (F). Data shown as mean ± SD; comparison by unpaired t test; *p < 0.05; **p < 0.01; ***p < 0.001; ****p < 0.0001. Remaining comparisons are non-significant.

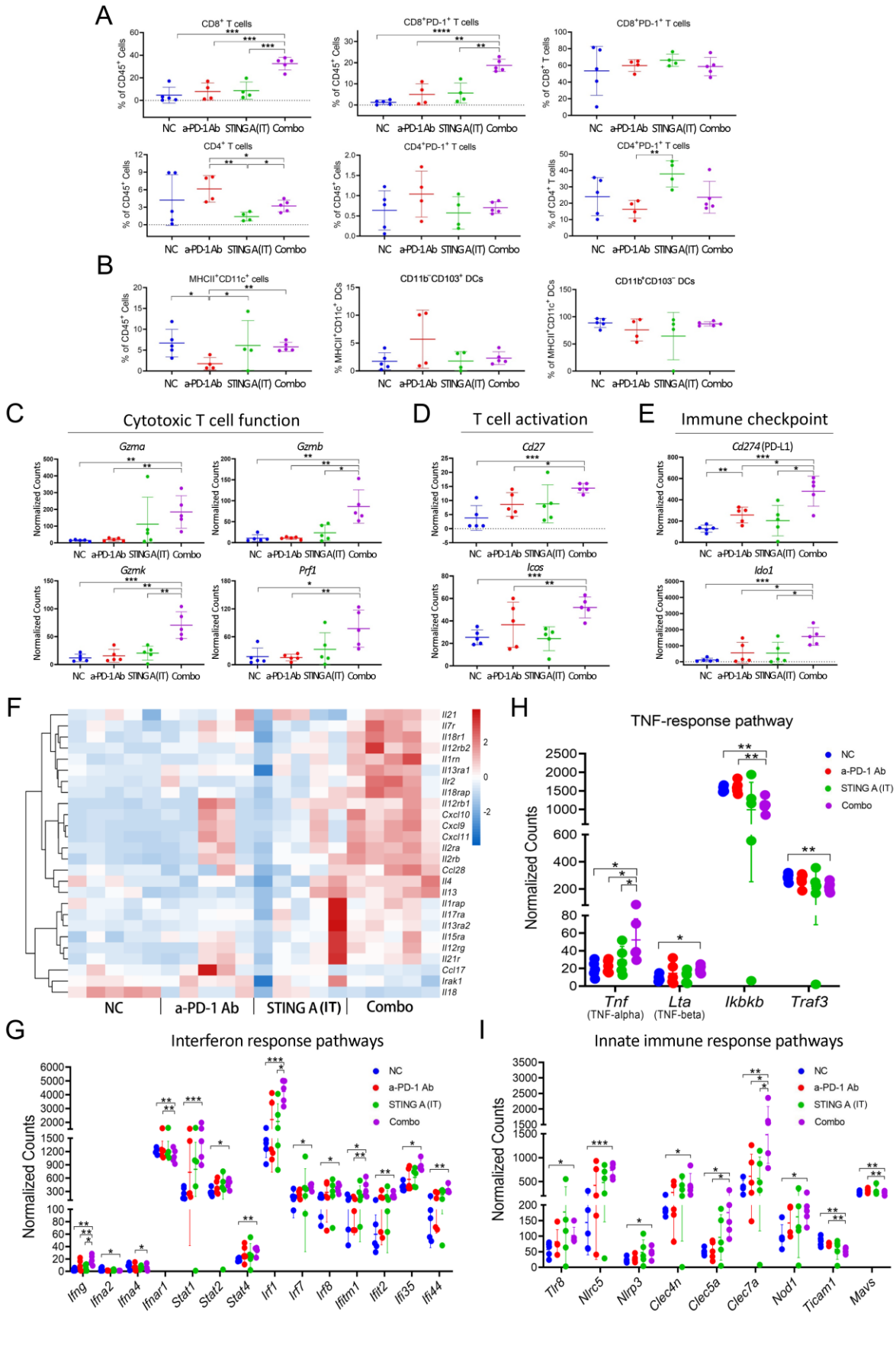
A
CD8+ T cells
CD8+PD-1+ T cells
CD8+PD-1+ T cells
CD4+ T cells
CD4+PD-1+ T cells
CD4+PD-1+ T cells
% of CD45+ Cells
% of CD8+ T cells
% of CD4+ T cells
NC a-PD-1Ab STINGA(IT) Combo
B
MHCII+CD11c+ cells
CD11b-CD103+ DCs
CD11b+CD103- DCs
% of MHCII+CD11c+ DCs
C
Cytotoxic T cell function
Gzma
Gzmb
Gzmk
Prf1
D
T cell activation
Cd27
Iccs
E
Immune checkpoint
Cd274 (PD-L1)
Ido1
Normalized Counts
F
Il21
Il7r
Il18r1
Il12rb2
Il1rn
Il13ra1
Il2r
Il18rap
Il12rb1
Cxcl10
Cxcl9
Cxcl11
Il2ra
Il2rb
Ccl28
Il4
Il13
Il1rap
Il17ra
Il13ra2
Il15ra
Il12rg
Il21r
Ccl17
Irak1
Il18
NC
a-PD-1 Ab
STING A (IT)
Combo
H
TNF-response pathway
Tnf (TNF-alpha)
Lta (TNF-beta)
Ikbkb
Traf3
G
Interferon response pathways
Ifng
Ifna2
Ifna4
Ifnar1
Stat1
Stat2
Stat4
Irf1
Irf7
Irf8
Ifitm1
Ifit2
Ifi35
Ifi44
I
Innate immune response pathways
Tlr8
Nlrc5
Nlrp3
Clec4n
Clec5a
Clec7a
Nod1
Ticam1
Mavs

Figure 4. STING agonist in combination with anti-PD-1 antibody enhances the infiltration and activation of effector T cells in the distant subcutaneous tumors. (A) Percentages of immune cells in the remote SubQ tumors, such as the $CD8^+$, $CD8^+PD\text{-}1^+$, $CD4^+$, and $CD4^+PD\text{-}1^+$T cells among $CD45^+$leucocytes, the $CD8^+PD\text{-}1^+$among $CD8^+$T cells, and the $CD4^+PD\text{-}1^+$T cells among $CD4^+$T cells, respectively. (B) Percentages of the $MHCII^+CD11c^+$DC, $CD11b^-CD103^+$ and $CD11b^+CD103^-$ DC subtypes DC among $CD45^+$leucocytes, respectively, in the distant SubQ tumors. Differentially expressed genes in the distant SubQ tumors from different treatment groups, including those in the gene families of cytotoxic T cell function (C), T cell activation (D), and the immune checkpoint activators (E). (F) Heatmap of the interleukin family genes and chemokine genes that were significantly increased in the Combo group comparing to the vehicle control treatment group. (G) Expression of genes in the IFN-response pathways in SubQ tumors from different treatment groups. (H) Expression of genes in the TNF-response pathways in SubQ tumors from different treatment groups. (I) Expression of genes in the innate immune response pathways in SubQ tumors from different treatment groups. Data shown as mean ± SD; comparison by unpaired t test; *$p < 0.05$; **$p < 0.01$; ***$p < 0.001$; ****$p < 0.0001$. Remaining comparisons are non-significant.

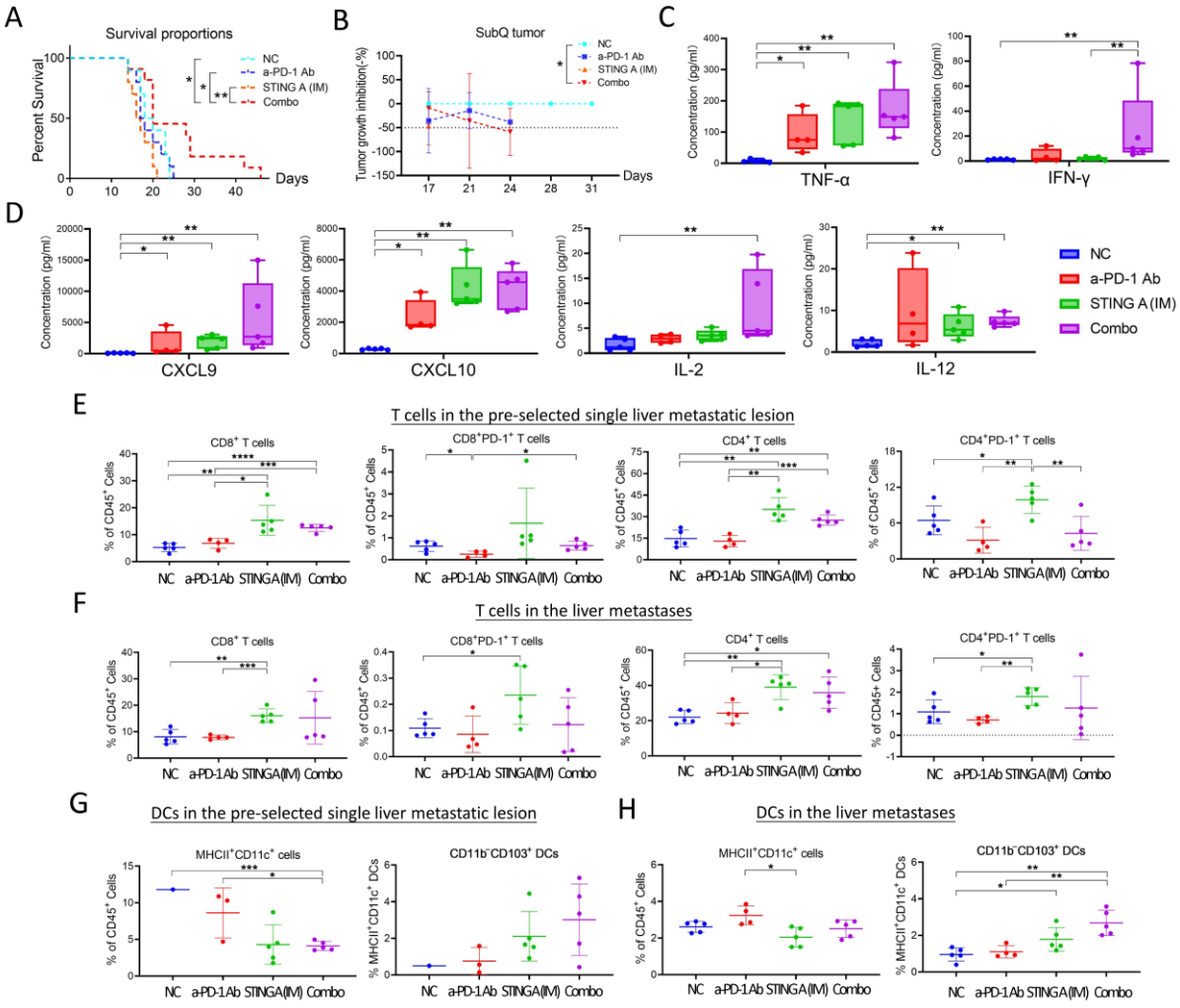

Figure 5. Intramuscular injection of STING agonist in combination with anti-PD-1 antibody prolonged the survival of liver metastasis mice and induces both systemic and intratumoral immune response. (A) Kaplan-Meier's survival curves compare the survival in different intratumoral (IM) treatment groups. (B) TGI on distant SubQ tumors. Dashed line at -50% indicates statistically significant inhibition. (C) Comparison of serum concentrations of TNF-α and IFN-γ collected 6 hours after the first IM injection between treatment groups. (D) Comparison of serum concentrations of CXCL9, CXCL10, IL-2, and IL-12 collected 6 hours after the first IM injection between treatment groups. Percentages of the $CD8^+$, $CD8^+PD\text{-}1^+$, $CD4^+$, and $CD4^+PD\text{-}1^+$T cells among $CD45^+$leucocytes in the pre-selected, target single liver metastatic lesions (E) and non-target liver metastases (F). Percentages of the $MHCII^+CD11c^+$DC and $CD11b^-CD103^+$subtype among $CD45^+$leucocytes, respectively, in the pre-selected single liver metastatic lesion (G) and non-target liver metastases (H). Data shown as mean ± SD; comparison by Log-rank test for A and by unpaired t test for others; *p < 0.05; **p < 0.01; ***p < 0.001; ****p < 0.0001. Remaining comparisons are non-significant.

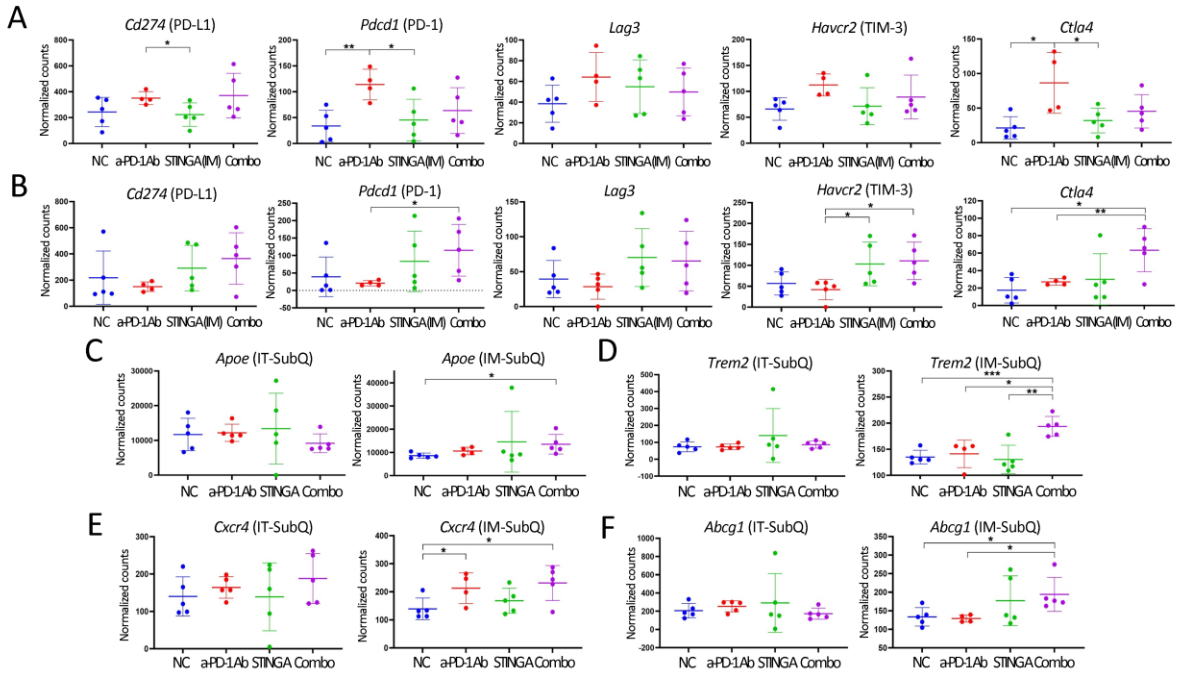

Figure 6. Comparison of expressions of differentially expressed genes in tumors from systemically treated mice. Expression of genes of the checkpoint gene family in pre-selected, target single liver metastatic lesions (A) and distant subcutaneous tumors (B) from the intramuscularly treated mice. Expression of *Apoe* (C), *Trem2* (D), *Cxcr4* (E), and *Abcg1* (F) in the distant subcutaneous tumors from both intratumoral and intramuscularly treated mice. Data shown as mean ± SD; comparison by unpaired t test; *p < 0.05; **p < 0.01; ***p < 0.001. Remaining comparisons are non-significant.

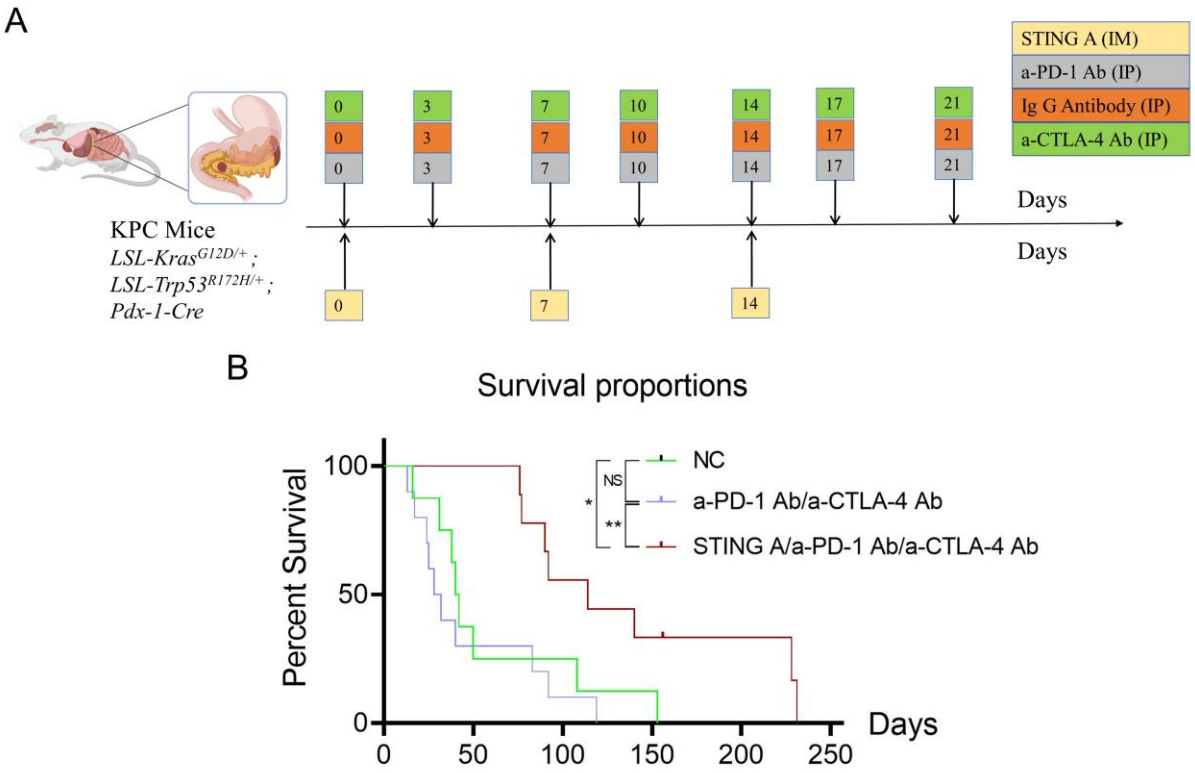

Figure 7. STING agonist in combination with immune checkpoint inhibitors significantly improved the survival of genetically engineered KPC mice. (A) Treat schema. (B) Kaplan-Meier survival curves compare overall survival between different treatment groups. NC, vehicle/isotype antibody control; STING A, STING agonist; a-PD-1 Ab, anti-PD-1 antibody; a-CTLA-4 Ab, anti-CTLA-4 antibody; IM, intramuscular; IP, intra-peritoneal. Data shown as mean ± SD; comparison by Log-rank test; *p < 0.05; **p < 0.01; NS, not significant.